

HIGH RESOLUTION RANGE PROFILE IDENTIFYING SIMULATION OF LASER RADAR BASED ON PULSE BEAM SCATTERING CHARACTERISTICS OF TARGETS

M.-J. Wang

Institute of E.M. Wave Propagation & Scattering
Xianyang Normal College
Box 103, 712000, China

Z.-S. Wu

Science School
Xidian University
Box 273, 710071, China

Y.-L. Li

Institute of E.M. Wave Propagation & Scattering
Xianyang Normal College
Box 103, 712000, China

G. Zhang

Science School
Xidian University
Box 273, 710071, China

Abstract—This is a presentation of an innovative technique of rigid body estimation for use with laser high-range resolution profile (LHRRP) simulations. The theory of pulse beam scattering from random rough surface is used to build a theoretical model which computes simulations for the laser pulse HRRP of the whole dimension target. As two especial cases, the LHRRP of sphere and cone are simulated in detail. We discuss and analyze some influential factors on laser radar HRRP imaging such as their dimensions, correlation length and height root mean square of the rough surface, refractive index of the material and width pulse. The simulated results suggest that the

Corresponding author: M.-J. Wang (wmjxd@yahoo.com.cn).

reliable identifications are possible provided in some aero and aerial recognized applications with higher resolution by laser radar.

1. INTRODUCTION

The high resolution range profiles (HRRP) is the amplitude of the coherent summations of the complex time returns from scatterers in each range cell, which represents the projection of the complex returned echoes from the target scattering centers onto the radar line-of-sight (LOS), HRRP as feature vectors for radar target recognition are known to have many merits. It detects some information of target structure signatures such as, size, distance, attitude, scatterer distribution, etc. thereby radar HRRP target recognition has received intensive attention from the radar automatic target recognition (RATR) community, and many researchers have developed algorithms and experiments for recognizing objects from range images in radar application [1–7].

In recent years, with development of the laser technology, there has been an increasing interest in and need for investigation the laser radar to identify the target in civilian and aerospace fields [8–13]. So the laser high-range resolution profile (LHRRP) technologies will play an more and more important roles in target recognition and battle sense. As compared to HRRP radar image, LHRRP is easy to offer enough and precise data on Attitude characteristic determination of target such as ground-base, spacecraft and airplane [14–16]. As a result, Laser high range revolution imaging Radar is a novel technology, has particularly attracted the attention of a great many institutes [8–18].

The characteristics of electromagnetic wave scattering from targets establish a theoretic basis for studying radar HRRP target recognition, so some researchers are develop a great many electromagnetic scattering theories and methods on different targets [19–24]. However, comparison of simulation on radar HRRP and laser radar HRRP, it must be existed some differences by electromagnetic scattering theories. In order to obtain the laser radar HRRP of complex targets, the paper present a novel theoretical model of the pulse beam scattering from random rough surfaces, which based on the electromagnetic Gaussian beams scattering theories and its application [25–29].

The body of this paper proceeds as follows. In Section 2, the theoretical procedure for the determination of the laser radar of a pulse beam by an arbitrary scatterer is given. Section 3 provides the numerical simulation for the HRRP properties of a tightly focused Laser pulse beam normally incident on some typical targets such as a sphere, a cone et al.. The work is summarized in Section 4.

2. THE LASER RADAR EQUATION OF PULSE BEAM SCATTERING FROM AN ARBITRARY SCATTERED BODY

As computing the backward echo power of pulse beam scattering from scattered body, impulse response in time domain can be written [17, 18]

$$G(t) = G_c(t) + G_f(t) \quad (1)$$

The pulse coherent scattering power is obtained as:

$$G_c(t) = \Gamma_{c0}(\omega_0)H_c(t) \quad (2)$$

$$\Gamma_{c0}(\omega_0) = \frac{k_0^2 w_0^4 \sigma_g}{16\pi \rho_0^4} |R(0)|^2 |\chi(-2k_0)|^2 \exp\left[-\frac{k_0^2 w_0^2 g_0(\vec{r}'_0)}{2\rho_0^2}\right] \quad (3)$$

$$\begin{aligned} H_c(t) &= \frac{1}{2\pi} \int d\omega_d \exp\left[-\frac{w_0^2 g_0(\vec{r}'_0) \omega_d^2}{4\rho_0^2 c^2}\right] \exp(-2\omega_d^2 \sigma^2 / c^2) \exp(i\omega_d t') \\ &= \frac{1}{2\pi} \frac{\sqrt{\pi}}{\sqrt{A}} \exp(-t'^2 / 4A) \end{aligned} \quad (4)$$

where $t' = t - 2\rho_0/c + 2\hat{k}_s \cdot \vec{r}'_0/c$, $A = w_0^2 g_0(\vec{r}'_0)/4\rho_0^2 c + 2\sigma^2/c^2$. And pulse incoherent scattering power is given

$$G_f(t) = \frac{k_0^2 w_0^4}{16\pi \rho_0^4} \int dS' \exp\left[-\frac{k_0^2 w_0^2 g_0(\vec{r}')}{2\rho_0^2}\right] \sigma_p^0(\vec{r}') H_f(\vec{r}', t) \quad (5)$$

$$\begin{aligned} H_f(\vec{r}', t) &= \frac{1}{2\pi} \int d\omega_d \exp\left[-\frac{w_0^2 g_0(\vec{r}') \omega_d^2}{4\rho_0^2 c^2}\right] \exp(-q_z'^2 \sigma^2 \omega_d^2 / 2c^2) \\ &\quad \exp(i\omega_d t'') = \frac{1}{2\pi} \frac{\sqrt{\pi}}{\sqrt{B}} \exp(-t''^2 / 4B) \end{aligned} \quad (6)$$

where $q_z' = 2\hat{k}_s \cdot \hat{n}'(\vec{r}')$, $t'' = t - 2\rho_0/c + 2\hat{k}_s \cdot \vec{r}'/c$, $B = w_0^2 g_0(\vec{r}')/4\rho_0^2 c + q_z'^2 \sigma^2 / 2c^2$.

Let us suppose that $P_i(t)$ is the power signal of incident laser pulse, and width of pulse is T_0 . The laser pulse scattering from a complex target is shown in Fig. 1. The scattering power $P_s(t)$ can be expressed by convolution integral of formation $P_i(t)$, $G_c(t)$ and $G_f(t)$

$$P_s(t) = G_c(t) \otimes P_i(t) + G_f(t) \otimes P_i(t) = P_c(t) + P_f(t) \quad (7)$$

In Equation (7), $P_c(t)$ and $P_f(t)$ is the coherent and incoherent scattering power from complex body. Put the Equations (2) and (5) into (7), and consider some factors such as the aperture of detector,

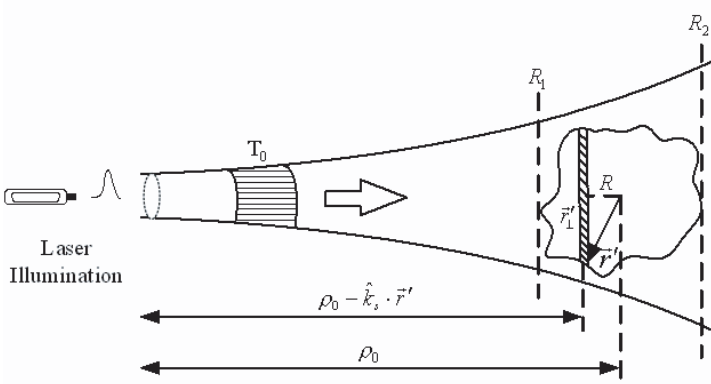


Figure 1. Scattering of pulse laser beam by object with complex target.

the optical efficiency, the emission and receiver system and attenuation along the propagation path of the echo laser pulse wave, so the laser radar equation of pulse beam scattering from arbitrary scattered body can be expressed [17, 18]

$$P_c(t) = \frac{P_i T_{A1} \eta_t}{\pi \phi^2 \rho_0^2} \pi w_0^2 \exp \left[-\frac{2g_0(\vec{r}'_0)}{\phi^2 \rho_0^2} \right] |R(0)|^2 |\chi(-2k_0)|^2 \sigma_g \frac{T_{A2}}{4\pi \rho_0^2} \frac{\pi D^2 \eta_r}{4} \quad (8)$$

$$P_f(t) = \int dS' \frac{P_i T_{A1} \eta_t}{\pi \phi^2 \rho_0^2} \pi w_0^2 \exp \left[-\frac{2g_0(\vec{r}')}{\phi^2 \rho_0^2} \right] \sigma_p^0(\vec{r}') \frac{T_{A2}}{4\pi \rho_0^2} \frac{\pi D^2 \eta_r}{4} \quad (9)$$

In Equations (8) and (9), T_{A1} , T_{A2} is the rate of the average atmospheric transmission from the laser illumination and the receiver to scattered body respectively. η_t , η_r is the Equivalent optical efficiency the emission and receiver system, $\phi = 2/k_0 w_0$ is the width of pulse, D is the aperture of detector, ρ_0 is the detected distance and w_0 is beam waist radius. Combine Equations (8) with (9) in Equation (7), the scattering power of arbitrary scattered body is given as following:

$$P(t) = \int dS' \frac{P_i T_{A1} \eta_t}{\pi \phi^2 \rho_0^2} \pi w_0^2 \exp \left[-\frac{2g_0(\vec{r}')}{\phi^2 \rho_0^2} \right] \sigma(\vec{r}') \frac{T_{A2}}{4\pi \rho_0^2} \frac{\pi D^2 \eta_r}{4} \quad (10)$$

where $\sigma(\vec{r}')$ is pulse beam scattered cross section, it include two parts, coherent scattered section $\sigma_c(\vec{r}') = |R(0)|^2 |\chi(-2k_0)|^2 \sigma_g \delta(\vec{r}' - \vec{r}'_0)$ and incoherent scattered section $\sigma_p^0(\vec{r}')$. The formation of Equation (10)

show that the total scattering power is the summation power of scattering point on the surface of complex target, and the power scattering point still contain coherent and incoherent component.

3. THE NUMERICAL SIMULATION FOR THE LASER PULSE HRRP IMAGING CHARACTERISTIC

As an application, we choose two kinds of typical scattered bodies, sphere and cone, discuss and analyze their dimensions, correlation length and height root mean square of rough surface, the complex refractive index of their material, and other the influence factors for laser radar HRRP imaging.

Geometric model of laser pulse scattering from a sphere is shown in Fig. 2. It is supposed that the sphere whose center is located at the origin of the coordinate system $OXYZ$, with a being its radii and laser pulse incidence along Z axis, laser wavelength $\lambda = 1.06 \mu\text{m}$. According to Equation (7), the analytic expression of scattering power of a sphere is written:

$$P(t) = \int_0^a \int_0^{2\pi} ad\varphi dz \frac{P_i(t - 2\rho_0/c + 2z/c)T_{A1}\eta_t}{\pi\phi^2\rho_0^2} \pi w_0^2 \exp\left[-\frac{2(a^2 - z^2)}{\phi^2\rho_0^2}\right] \times \sigma(\vec{r}') \frac{T_{A2}}{4\pi\rho_0^2} \frac{\pi D^2\eta_r}{4} \quad (11)$$

Due to the symmetry of the sphere, the scattering power and cross section haven't any relation to and so azimuth φ , the Equation (11) is

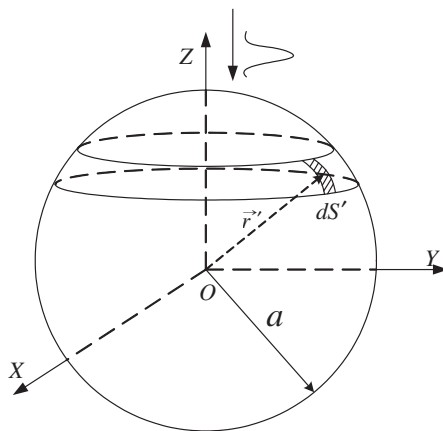


Figure 2. Geometry of laser pulse scattering from a sphere.

rewritten as:

$$P(t) = \int_0^a adz \frac{P_i(t - 2\rho_0/c + 2z/c)T_{A1}\eta_t}{\pi\phi^2\rho_0^2} \pi w_0^2 \exp\left[-\frac{2(a^2 - z^2)}{\phi^2\rho_0^2}\right] \times 2\pi\sigma(z) \frac{T_{A2}}{4\pi\rho_0^2} \frac{\pi D^2\eta_r}{4} \quad (12)$$

In order to validate our theory and simulated methods, we compare our results with the radar HRRP in [2] are shown in Fig. 3. The frequency electromagnetic (EM) wave $f = 3$ GHz (S-band) in [2], and the width of laser pulse $wP = 1$ ns, the laser HRRP of a sphere whose radii $a = 1.0$ m.

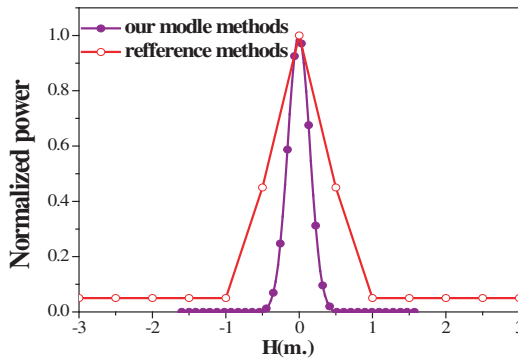


Figure 3. LHRRP imaging of sphere compare with that of radar HRRP imaging in [2].

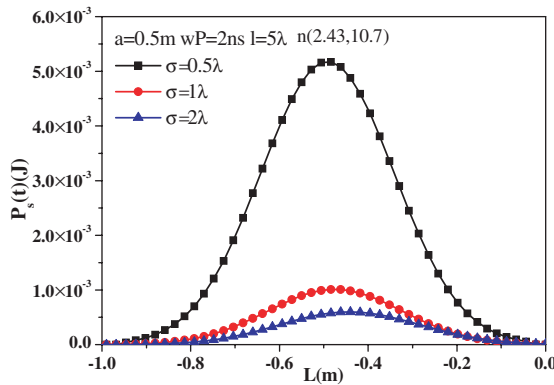


Figure 4. LHRRP image of a sphere with rough surface in different height root mean square.

Comparing two cure lines of the sphere radar and laser radar HRRP imaging characteristic as the simulation results, it is found that laser HRRP has the same trend with the radar HRRP, but the former decrease faster than the latter in the same scattering points. The main reasons have two aspects, on one hand, the laser wavelength is far less than the EM wavelength, which results in a higher resolution ratio, on the other hand, the scattering coherent component has a stronger influence on the laser than that of EM wave.

LHRRP image of a sphere with rough surface in different height root mean square $\sigma = 0.5\lambda, 1\lambda, 2\lambda$ is shown in Fig. 4, and given the radii of sphere $a = 0.5\text{ m}$, width laser pulse $wP = 2\text{ ns}$, correlation length of rough surface $l = 5\lambda$, complex refractive index of a

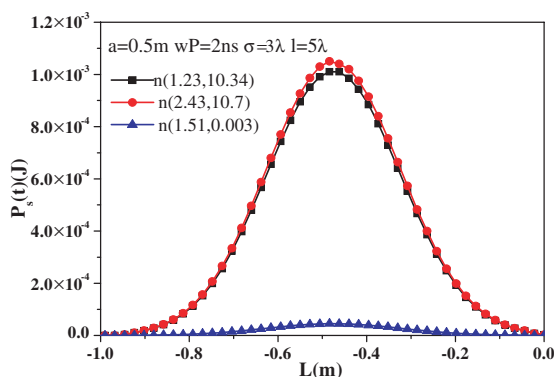


Figure 5. LHRRP image of a sphere with different complex refractive index.

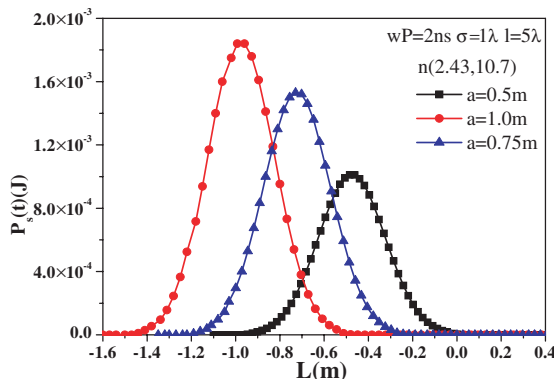


Figure 6. LHRRP image of a sphere with different radius.

material $n = 2.43 + 10.7i$. In Figs. 5 and 6, the LHRRP image of a sphere change with three kinds of different complex refractive index of materials and radials. In Fig. 5 the complex refractive index respectively is equal to $2.43 + 10.7i$, $1.23 + 10.34i$, $1.51 + 0.003i$ and the LHRRP of sphere with radii $a = 0.5, 0.75, 1.0$ m as shown In Fig. 6.

From the Figs. 4–6, it is found that LHRRP image of a sphere have the same distributed tendency, and the roughness of the surface, refractive index of the material, the radii of the sphere have influence on the echo scattering power value of LHRRP. The large roughness, small refractive index and radii correspond to the low echo scattering power value.

Due to the bottom surface of the cone being a plane, it hasn't a observable characteristic of LHRRP. So we consider an incident laser pulse beam propagating from the positive Z to the negative Z axis of the Cartesian coordinate system $OXYZ$, with the origin of the

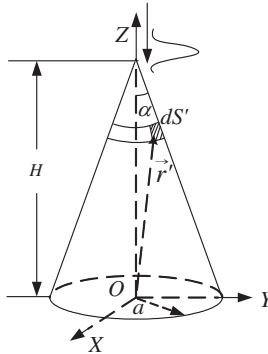


Figure 7. Geometry of laser pulse scattering from a cone.

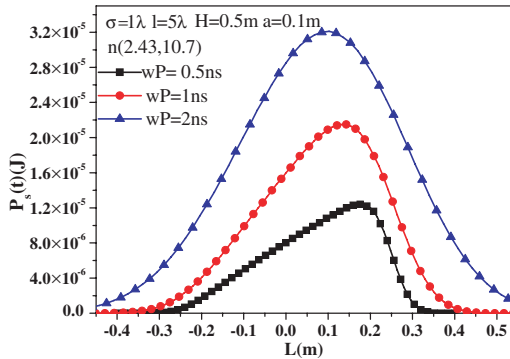


Figure 8. LHRRP image of a cone in different width laser pulse.

coordinate system is located at O , which is the center of the bottom surface, and a , α , H is the radii, apex angle and height of the cone. The Geometric relations of LHRRP simulation on a cone model of laser pulse scattering characteristics are shown in Fig. 7.

The LHRRP image of the cone with different laser width pulses (wP), radius of bottom surface and three kinds of similar shape are shown in Figs. 8 to 10. For the case wP = 0.5 ns, 1 ns, 2 ns from Fig. 8, we note that the width pulse is narrower and the simulation resolution of LHRRP is higher. As $H = 0.5$ m, the biggest scattering power value of a cone LHRRP images appear radii $a = 0.2$ m in Fig. 9. For three kinds of similar cones, their LHRRP images have the same characteristics as Fig. 10.

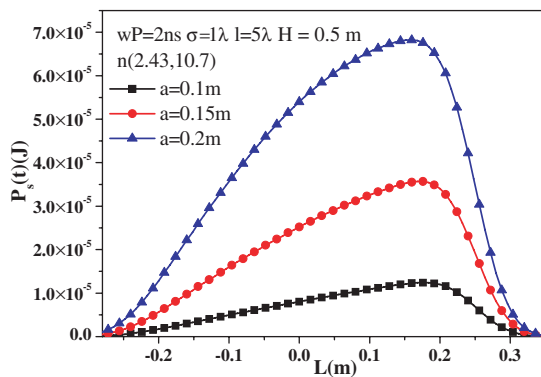


Figure 9. LHRRP image of a cone with in different radius of bottom surface.

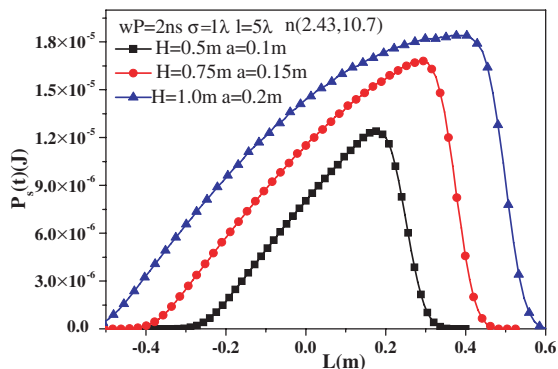


Figure 10. LHRRP image of three kinds similar shape cones.

4. CONCLUSION

In this paper, the analytical model of laser pulse HRRP image from arbitrary rough complex scattered bodies is built. We simulated two especial targets such as a sphere and a cone based on pulse beam scattering characteristics of targets. The influential factors on the LHRRP of sphere and cone are analyzed in detail. The simulated results show that the rough surface and the complex refractive index of material have an effect on the value of laser pulse scattered echo power, the width of incidence laser pulse effect on the revolution range image, and their structural or dimensional effect on the distributed characteristic of the LHRRP of a sphere and a cone. From the comparison of the LHRRP curves of sphere and cone, it is illustrated that LHRRP image of sphere is a symmetrical convex curves, and LHRRP image of cone is better shown in conical envelope curve, too. In addition, as the same height of the cone, the radii of the bottom surface is bigger, its LHRRP has a stronger scattering characteristic. If the cones have similar shapes, their LHRRP images have the same distributions. In a word, our works describe a novel method to simulated LHRRP images for a complex target, and establish a good foundation for micro-recognition with higher revolution by laser radar.

ACKNOWLEDGMENT

This works is supported by the National Natural Science Foundation of China (Grant No. 60801047, 60771038, 60741003) and the Natural Science Foundation of Shaanxi Province education office, China (Grant No. 08Jk480).

REFERENCES

1. Wehner, D. R., *High Resolution Radar*, 2nd edition, Artech House Artech House, Inc., Norwood, MA, 1994.
2. Andrews, A. K., "Computer and optical simulation of radar imaging systems," Doctor Dissertation, Washington State University, 1994.
3. Chen, V. C. and H. Ling, *Time-frequency Transforms for Radar Imaging and Signal Analysis*, Artech House, Boston, MA, 2002.
4. Bao, Z., M.-D. Xing, and T. Wang, *The Technology of Radar Image*, Publishing House of Electronics Industry, Beijing, 2004.
5. Skolnik, M. I., *Radar Handbook*, 3rd edition, McGraw-Hill Publishing Company, New York, 2008.

6. Atkins, R. G., R. T. Shin, and J. A. Kong, "A neural network method for high range resolution target classification," *Progress In Electromagnetics Research*, PIER 4, 255–292, 1991.
7. Deng, H. and H. Ling, "Clutter reduction for synthetic aperture radar imagery based on adaptive wavelet packet transform," *Progress In Electromagnetics Research*, PIER 29, 1–23, 2000.
8. Parker, J. K., E. B. Craig, D. L. Klick, et al., "Reflective tomography images from range-resolved laser radar measurements," *Applied Optics*, Vol. 27, 2642–2643, 1988.
9. Masters, L. T., M. B. Mark, and B. D. Duncan, "Range resolution enhancements for laser radar by phase modulation," *Aerospace and Electronics Proceedings of the IEEE*, 129–133, 1995.
10. Shirley, L. G. and G. R. Hallerman, "Applications of tunable lasers to laser radar and 3D imaging," MIT Lincoln Laboratory, Lexington Massachusetts, 1996.
11. Wei, G.-H. and P.-G. Yang, *Laser Technology Applying in Weapon Industry*, weapon industry publishing company, Beijing, 1999.
12. Gurdev, L. L., T. N. Dreischuh, and D. V. Stoyanov, "High-range-resolution velocity-estimation techniques for coherent doppler lidars with exponentially shaped laser pulses," *Applied Optics*, Vol. 41, 1741–1749, 2002.
13. Haridim, M., H. Matzner, Y. Ben-Ezra, and J. Gavan, "Cooperative targets detection and tracking range maximization using multimode ladar/radar and transponders," *Progress In Electromagnetics Research*, PIER 44, 217–229, 2004.
14. Matson, C. L., E. P. Magee, and D. H. Stone, "Reflective tomography for space object imaging using a short-pulse length laser," *Proc. SPIE*, Vol. 2302, 73–82, 1994.
15. Jacques, G. V. and L. D. Richard, "Model-based automatic target recognition system for forwardlooking groundbased and airborne imaging laser radars (LADAR)," *Proceedings of the IEEE*, Vol. 84, 126–163, 1996.
16. Yano, T., T. Tsujimura, and K. Yoshida, "Vehicle identification technique using active laser radar system," *IEEE Conference on Multisensor Fusion and Integration for Intelligent Systems*, 2003.
17. Chen, H., "Scattering of Gaussian beam by object with rough surface and its application on laser one-dimensional range profile," Doctoral Dissertation, Xidian University, 2004.
18. Wang, M.-J., "Research on scattering of pulse beam by target with rough surface and its laser range Doppler imaging," Doctoral Dissertation, Xidian University, 2008.

19. Li, Y.-L., M.-J. Wang, and G.-F. Tang, "The scattering from an elliptic cylinder irradiated by an electromagnetic wave with arbitrary direction and polarization," *Progress In Electromagnetics Research Letters*, Vol. 5, 137–149, 2008.
20. Ruppin, R., "Scattering of electromagnetic radiation by a coated perfect electromagnetic conductor sphere," *Progress In Electromagnetics Research Letters*, Vol. 8, 53–62, 2009.
21. Li, Y.-L., J.-Y. Huang, and M.-J. Wang, "Investigation of electromagnetic interaction between a spherical target and a conducting plane," *Journal of Electromagnetic Waves and Applications*, Vol. 21, No. 12, 1703–1715, 2007.
22. Li, Y.-L., J.-Y. Huang, M.-J. Wang, and S.-H. Gong, "The scattering cross section for a target irradiated by time-varying electromagnetic waves," *Journal of Electromagnetic Waves and Applications*, Vol. 21, No. 9, 1265–1271, 2007.
23. Li, Y.-L., J.-Y. Huang, and M.-J. Wang, "Scattering cross section for airborne and its application," *Journal of Electromagnetic Waves and Applications*, Vol. 21, No. 15, 2341–2349, 2007.
24. Li, Y.-L., J.-Y. Huang, and M.-J. Wang, "Investigation of electromagnetic complex scattering for conductor target based on electromagnetic images methods," *Journal of Electromagnetic Waves and Applications*, Vol. 21, No. 9, 1265–1271, 2007.
25. Wang, M.-J., Z.-S. Wu, and Y.-L. Li, "Investigation on the scattering characteristics of Gaussian beam from two dimensional dielectric rough surfaces based on the Kirchhoff approximation," *Progress In Electromagnetics Research B*, Vol. 4, 223–235, 2008.
26. Tuz, V. R., "Three-dimensional Gaussian beam scattering from a periodic sequence of Bi-isotropic and material layers," *Progress In Electromagnetics Research B*, Vol. 7, 53–73, 2008.
27. Dahl, M., "Electromagnetic Gaussian beams and Riemannian geometry," *Progress In Electromagnetics Research*, PIER 60, 265–291, 2006.
28. Wu, Z. and L. Guo, "Electromagnetic scattering from a multilayered cylinder arbitrarily located in a Gaussian beam, a new recursive algorithms," *Progress In Electromagnetics Research*, PIER 18, 317–333, 1998.
29. Shen, T., W. Dou, and Z. Sun, "Gaussian beam scattering from a semicircular channel in a conducting plane," *Progress In Electromagnetics Research*, PIER 16, 67–85, 1997.